A Train-Like Extreme Multiple Tropical Cyclogenesis Event in the Northwest Pacific in 2004

Kaiming Hu[1] (ID), **Johnny C. L. Chan[2]** (ID), **Gang Huang[1]** (ID), **Guanghua Chen[1]** (ID), **and Wei Mei[3]**

[1]State key Laboratory of Numerical Modeling for Atmospheric Sciences and Geophysical Fluid Dynamics and Center for Monsoon System Research, Institute of Atmospheric Physics, Chinese Academy of Sciences, Beijing, China, [2]Guy Carpenter Asia-Pacific Climate Impact Centre, School of Energy and Environment, City University of Hong Kong, Hongkong, [3]Department of Marine Sciences, University of North Carolina at Chapel Hill, Chapel Hill, NC, USA

Abstract Using observed data sets, an unprecedented multiple tropical cyclogenesis event over the northwest Pacific is identified, with seven tropical cyclones forming in sequence from 6 August to 10 September 2004. In this event, the preexisting tropical cyclones (TCs) generated the alternating cyclonic and anticyclonic disturbances in their wake region by exciting Rossby waves. The cyclonic disturbances subsequently intensified into new TCs within the monsoon trough, which was likely enhanced by anomalous warming in the tropical central Pacific and cooling in the tropical Indian Ocean, so that it lasted long enough to allow seven TCs to develop consecutively. An analysis of the historical records during 1979–2014 substantiates such linkage of the occurrence of this extreme multiple tropical cyclogenesis event to the anomalous sea surface temperature pattern and the monsoon trough. This result has important implications regarding the prediction of the multiple cyclogenesis events.

Plain Language Summary Tropical cyclones (TCs) are severe weather phenomenon, with important role in modulating regional and global climate. TC-induced extreme events often bring huge disasters to human society. This study has identified a hitherto unreported extreme event that seven TCs clustered together over the northwest Pacific in the late summer of 2004. The number of TCs in this event is the highest among the recorded multiple tropical cyclogenesis events (MTCEs). This study shows that the occurrence of this extreme MTCE is partly caused by the anomalous warming in the tropical central Pacific and cooling in the tropical Indian Ocean in the summer of 2004. Historical record further confirms that the anomalous sea surface temperature pattern increases the possibility in the occurrence of MTCEs. The result has important implications to improve the prediction skill of extreme MTCEs.

1. Introduction

Observations show that tropical cyclone (TC) activities tend to cluster in some active periods (Gray, 1979). When two or more TCs form within a relatively short period, it is commonly referred to as a multiple tropical cyclogenesis event (MTCE; Krouse & Sobel, 2010; Li & Fu, 2006). The spatiotemporal separation between TCs during MTCEs is consistent among different basins, with a median zonal distance between TCs of ~1640–2010 km and a median temporal separation between TC formations at 3–3.25 days (Schenkel, 2016, 2017). Previous studies have suggested that Rossby waves radiated from a preexisting TC contribute to a substantial fraction of MTCEs (Krouse & Sobel, 2010; Li & Fu, 2006; Schenkel, 2016; Shi et al., 2017). In the presence of a large-scale planetary vorticity gradient, a TC could excite alternating anticyclonic and cyclonic vorticity perturbations in its wake region by emitting Rossby wave energy (Chan & Williams, 1987; Ge et al., 2007; Holland, 1995; Krouse et al., 2008; Shi et al., 2016). The resulting cyclonic perturbations have the potentials to develop into new TCs and hence a MTCE (Holland, 1995; Li & Fu, 2006). Over the northwest Pacific (NWP), approximately 20–30% of TC formations are likely caused by Rossby wave dispersion from preexisting TCs (Fu et al., 2007; Xu et al., 2013).

A number of previous studies have shown that TC energy dispersion (TCED)-induced cyclogenesis is favored by environmental factors including easterly vertical shear, zonal convergence of low-level wind field, cyclonic low-level horizontal shear, and high moisture in the middle troposphere (Gao & Li, 2011; Ge et al., 2007; Krouse & Sobel, 2010). These factors help TC-induced wave energy accumulate in the lower troposphere that further spawn new TCs (Ge et al., 2007; Molinari et al., 2007; Webster & Chang, 1988). If the environmental
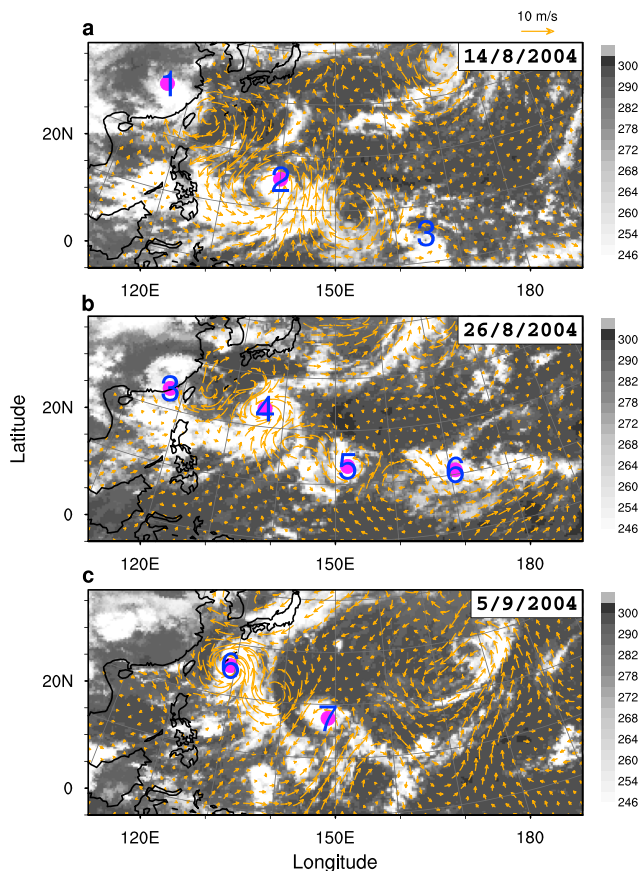
Figure 1. The 3- to 8-day filtered 10-m winds (vectors, from Cross-Calibrated, Multi-Platform) and brightness temperatures (grays, K, from Cloud Archive User Service) at UTC 00 on 14 August (a), 26 August (b), and 5 September (c) 2004. The vector scale is given on the upper right. The blue text represents the sequence of the TCs (1: Rananim, 2: Megi, 3: Aere, 4: Chaba, 5: unnamed tropical storm, 6: Songda, and 7: Sarika), and the magenta dots represent the locations of the tropical cyclones.

conditions allow the succession of TC-induced cyclogenesis, an extreme MTCE consisting of much more than two TCs is anticipated. So far, few studies have been devoted to addressing the possibility of the existence of such extreme MTCEs.

This study identifies a hitherto unreported extreme MTCE with seven TCs forming in sequence over the NWP in 2004, which include five typhoons: Rananim, Megi, Aere, Chaba, and Songda, a named tropical storm Sarika, and an unnamed tropical storm. The number of TCs in this event is the highest among all reported MTCEs in previous literatures. Three of the TCs made landfall in Japan and two in China, causing huge damage (Kim et al., 2005). This study also analyzed the characteristics of this extreme MTCE and the relevant environmental condition.

2. Data and Methods

The tracks of the TCs utilized in the present study are provided by Joint Typhoon Warning Center in the International Best Track Archive for Climate Stewardship version v03r09 (Knapp et al., 2010). The cloudiness is represented by the brightness temperature from the Cloud Archive User Service of the European Union (Hodges et al., 2000), with a spatial resolution of 0.33° latitude × 0.33° longitude and a 3-hourly temporal resolution. The 10-m winds associated with TCs are derived from the Cross-Calibrated, Multi-Platform (CCMP) Ocean Surface Wind Velocity (Atlas et al., 2011), which are available from 1991 to 2009 with a global spatial resolution of 0.25° latitude × 0.25° longitude and a 6-hourly temporal resolution in oceans. The CCMP is chosen due to its high spatial resolution compared with other observed data sets. To examine the synoptic-scale wind structures associated with TCs, a band-pass Lanczos filtering method (Duchon, 1979) is used to retain the 3- to 8-day signals (Lau & Lau, 1992) for the 10-m winds.

The 2.5° latitude × 2.5° longitude daily National Centers for Environmental prediction's (NCEP-DOE) version 2 Reanalysis (Kanamitsu et al., 2002) and the 1° latitude × 1° longitude monthly Hadley Center sea surface temperature (SST; Rayner et al., 2003) over 1979–2014 are used to provide environmental data for examining the factors generally considered to be favorable for MTCE occurrences: low-level circulation, zonal convergence of low-level wind field, vertical shear, and the field of TC genesis potential index (Camargo et al., 2007). Zonal vertical wind shear is represented by the difference of zonal winds between 200 and 850 hPa. To reduce the effect of the TCs on the environmental factors, all signals with periods shorter than 8 days are removed using a low-pass Lanczos filter (Duchon, 1979).

The present study utilizes two types of statistical significance tests including the following: (1) a 2000-sample bootstrap approach (Johnson, 2001) with replacement for a two-tailed test to determine whether the environmental variables during the late summer of 2004 are significantly different from their climatology during 1979–2014 and (2) a two-tailed Student's t test to evaluate the significances of the composite, regression, and correlation analyses.

3. Results

Figure 1 shows the brightness temperature and the 3- to 8-day filtered 10-m winds associated with the MTCE in 2014. On 14 August, Typhoon Rananim made landfall in China, followed by a sequence of anticyclonic and cyclonic perturbations in its wake. In the following days, Typhoons Megi, Aere, and Chaba, an unnamed tropical depression, Typhoon Songda, and tropical storm Sarika developed within the cyclonic perturbations. Five of the seven TCs formed one after the other with a mean temporal separation of ~5.8 days, while two TCs Aere and Chaba formed at almost the same time on 17 August (Figure S1 in the supporting
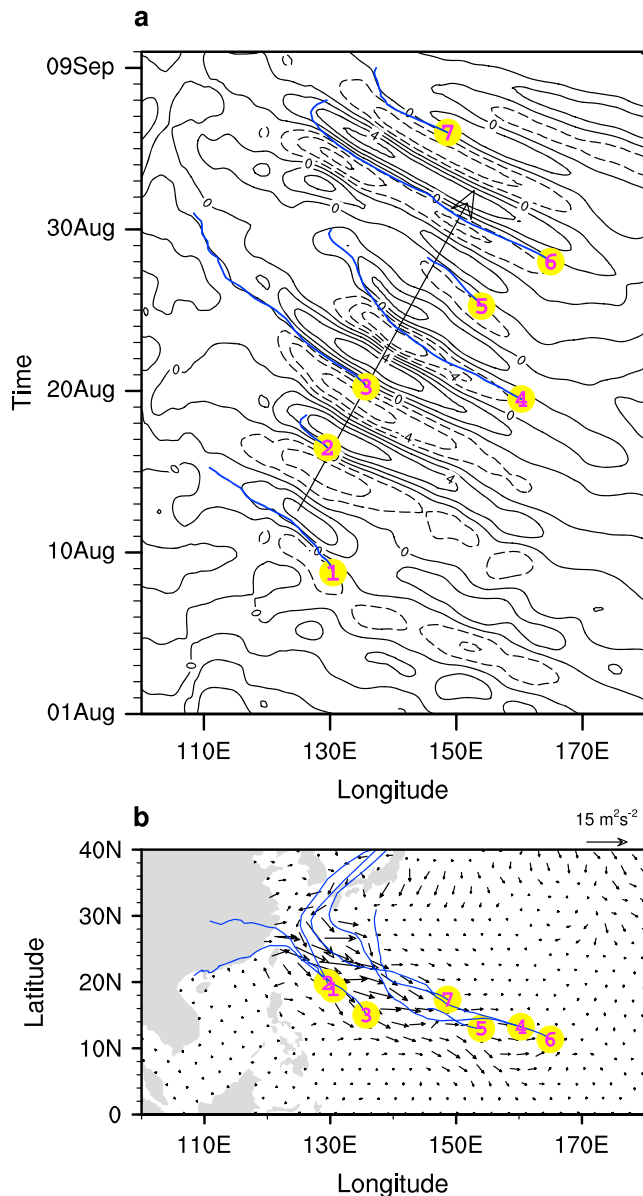
Figure 2. Wave structure of the MTCE. (a) Hovmöller diagram of the 3- to 8-day filtered 10-m meridional winds, averaged over 5–25°N, for the period of 1 August to 10 September 2004. Contour interval is 2 m/s. (b) The horizontal component of local *EP* vectors over 1 August to 9 September 2004. The red text represents the sequence of the TCs (1: Rananim, 2: Megi, 3: Aere, 4: Chaba, 5: unnamed TS, 6: Songda, and 7: Sarika), and the yellow dots represent the origins of the TCs identified by when the maximum sustained wind gust (10 min) first exceeding 35 kt. The blue lines represent the TC tracks. The long arrow in (a) denote the direction of group velocity. MTCE = multiple tropical cyclogenesis event.

information). From the beginning of Typhoon Rananim on 6 August to the end of Sarika on 10 September, this MTCE lasted for around 35 days. The seven TCs moved northwestward together in a train-like manner over the NWP.

Figure 2a shows the Hovmöller diagram of the 10-m 3- to 8-day filtered meridional winds, averaged between 5° and 25°N, over the NWP from 1 August to 10 September 2004. A prominent wave packet can be identified with an amplitude of approximately 6 m/s in the meridional wind. The average zonal wavelength and period of the Rossby wave train (Figure 2a) are estimated by the distance and time between the consecutive maxima or minima in the meridional wind, which are of ~2,469 km and 5.2 days, respectively. The zonal wavelength is comparable to that in a TCED case in August 2000 (Li & Fu, 2006). According to Figure 2a (see black arrow), the mean zonal phase velocity is of ~ −5.5 m/s and the mean zonal group velocity is ~ 1.7 m/s, suggesting that it is a Rossby wave packet. The wave packet began on 6 August along with the formation of Typhoon Rananim and ended on 10 September with the demise of tropical storm Sarika. All the seven TCs formed (yellow dots) inside this wave packet.

To demonstrate the Rossby wave energy dispersion of this wave packet, we calculated the horizontal local Eliassen-Palm (*EP*) vector (Li & Fu, 2006; Trenberth, 1986) during the period of 5 August to 10 September 2004. Here local $EP = \left(\frac{[-u'u'+v'v']}{2}, [-u'v'] \right)$, where [ ] represents the time average between 5 August and 10 September and u′ and v′ are the zonal and meridional components of the 3- to 8-day filtered 10-m wind perturbations from CCMP, respectively. In agreement with the wave packet, there are significant southeastward local EP fluxes along a channel from the region between Taiwan and Japan to the equatorial central Pacific (Figure 2b). These results suggest that the seven TCs and the wave packet may be coupled with each other.

One intriguing issue arises as to why this MTCE can last for such a long time. At 850 hPa, the low-pass wind anomalies (with period >8 days) during 5 August to 10 September 2004 featured a strong monsoon trough extending from the region between Taiwan and Japan to the tropical central Pacific (Figure 3a). Associated with the trough, the genesis potential index is above normal (Figure 3b), the zonal winds show an easterly shear (Figure 3c), and the convergence of the 850-hPa zonal winds (Figure 3d) is enhanced in the trough region. All of these factors provide favorable conditions that allow the TC-induced cyclonic disturbances to develop into the new TCs (Gao & Li, 2011; Ge et al., 2007; Krouse & Sobel, 2010; Molinari et al., 2007; Webster & Chang, 1988). This strong and long-lasting monsoon trough, together with the long-lasting wave train, allows the seven TCs to form in sequence.

In the summer of 2004, positive and negative SST anomalies developed in the tropical central Pacific and most of the tropical Indian Ocean, respectively (Figure 4a). Such an anomalous SST pattern is generally considered to be favorable for the development of an anomalous monsoon trough over the NWP (Wang et al., 2003; Xie et al., 2009). To confirm the role of SST anomalies in the monsoon trough, two numerical experiments were conducted based on an atmospheric general circulation model (AGCM). One (EXP1) is forced by the observed monthly SST in 2004 and climatological sea ice and the other (EXP2) is forced by the climatological monthly SST and sea ice. In each experiment, the model is integrated for 20 years. The AGCM used is the fifth Hamburg version of the European Centre for Medium-Range Weather
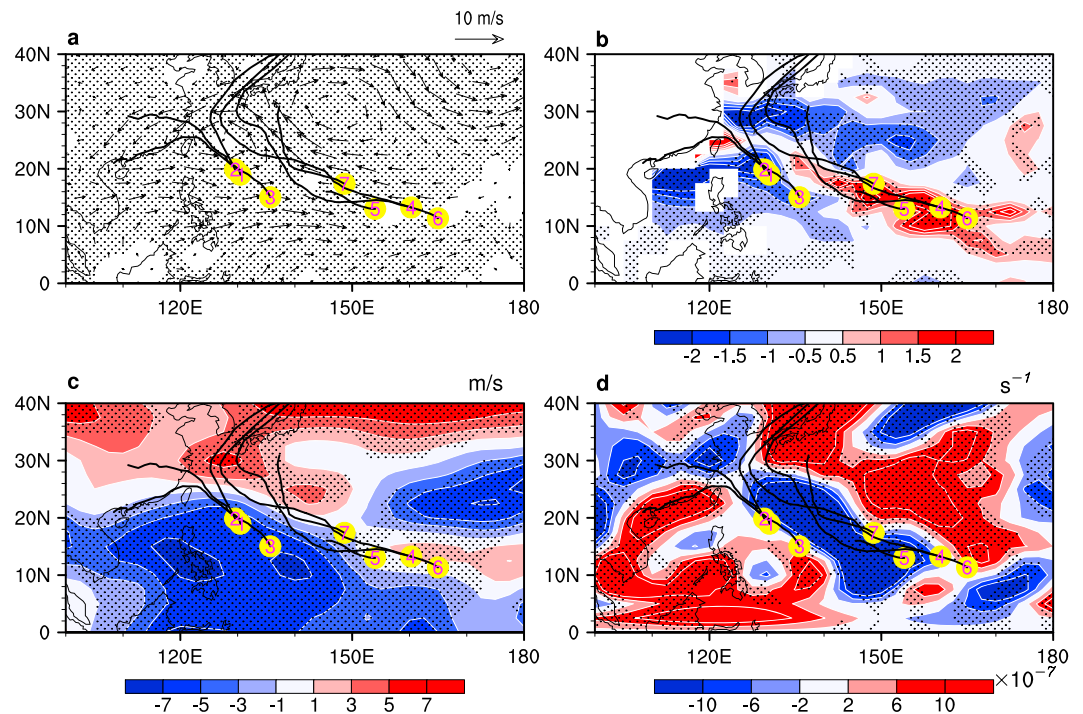
Figure 3. (a) The low-pass (with period >8 days) wind anomalies at 850 hPa, (b) GPI, (c) vertical zonal wind shear (U200–U850; m/s), (d) divergence of 850-hPa zonal winds (s^{-1}) during 5 August to 10 September 2004 compared with climatology (1979–2014). The red text represents the sequence of TCs (1: Rananim, 2: Megi, 3: Aere, 4: Chaba, 5: unnamed TS, 6: Songda, and 7: Sarika), and the yellow dots denote the genesis location of the TCs identified by when the maximum sustained wind gust (10 min) first exceeding 35 kt. The black lines represent the TC tracks. Shading denotes the anomalies passing the 95% confidence level based on the 2000-sample bootstrap test. TC = tropical cyclone; TS = tropical storm.

Forecasts model (ECHAM5; Roesch & Roeckner, 2006) with triangular truncation at zonal wavenumber 63 and 19 levels in the vertical.

Composite differences in mean 850-hPa circulation over JJAS (June to September) between EXP1 and EXP2 show prominent westerly anomalies over the equatorial western Pacific and cyclonic anomalies over the NWP (Figure 4b), similar to those in the observations (Figure 4a). Even in the relatively short period from 5 August to 10 September, the AGCM simulations (Figures 4c–4e) also broadly reproduce the observed enhanced monsoon trough, easterly vertical shear, and low-level zonal wind convergence over the NWP (Figure 3). The consistency between model simulations and observation demonstrates that the SST pattern appears to be important in forming the long-lasting monsoon trough. Note that the observed circulation anomalies in the summer of 2004 do not always show a monsoon trough over the NWP (Figure S2). The intra-seasonal suppression and enhancement of the monsoon trough maybe associated with the Madden-Julian Oscillation (Nakazawa, 2006). In August 2004 (Figure S3), the Madden-Julian Oscillation is in its positive phase over the western Pacific (Wheeler & Hendon, 2004), which may also contribute to enhancing the monsoon trough. As SST has a long-term predictability, this study mainly focuses on the role of the SST pattern in the MTCE occurrence.

To investigate whether the relation between the SST pattern and MTCE also exists in other years, we further examined each TC's life span from 1979 to 2014 using the 6-hr International Best Track Archive for Climate Stewardship data set. If a new TC appears to the southeast of the previous TC, the distance of two TCs is less than 3,500 km, and the area mean of the zonal value of instantaneous local EP fluxes in the wake region of the previous TC is above 1 m^2/s^2; this new TC is considered as one generated by TCED. Here the wake region is defined as a 5° latitudes × 10° longitudes region to the southeast of the TC. The result is not sensitive to the selection of EP value, when its value ranges from 0.5 to 5 m^2/s^2. The selection of 3,500 km as the cutoff
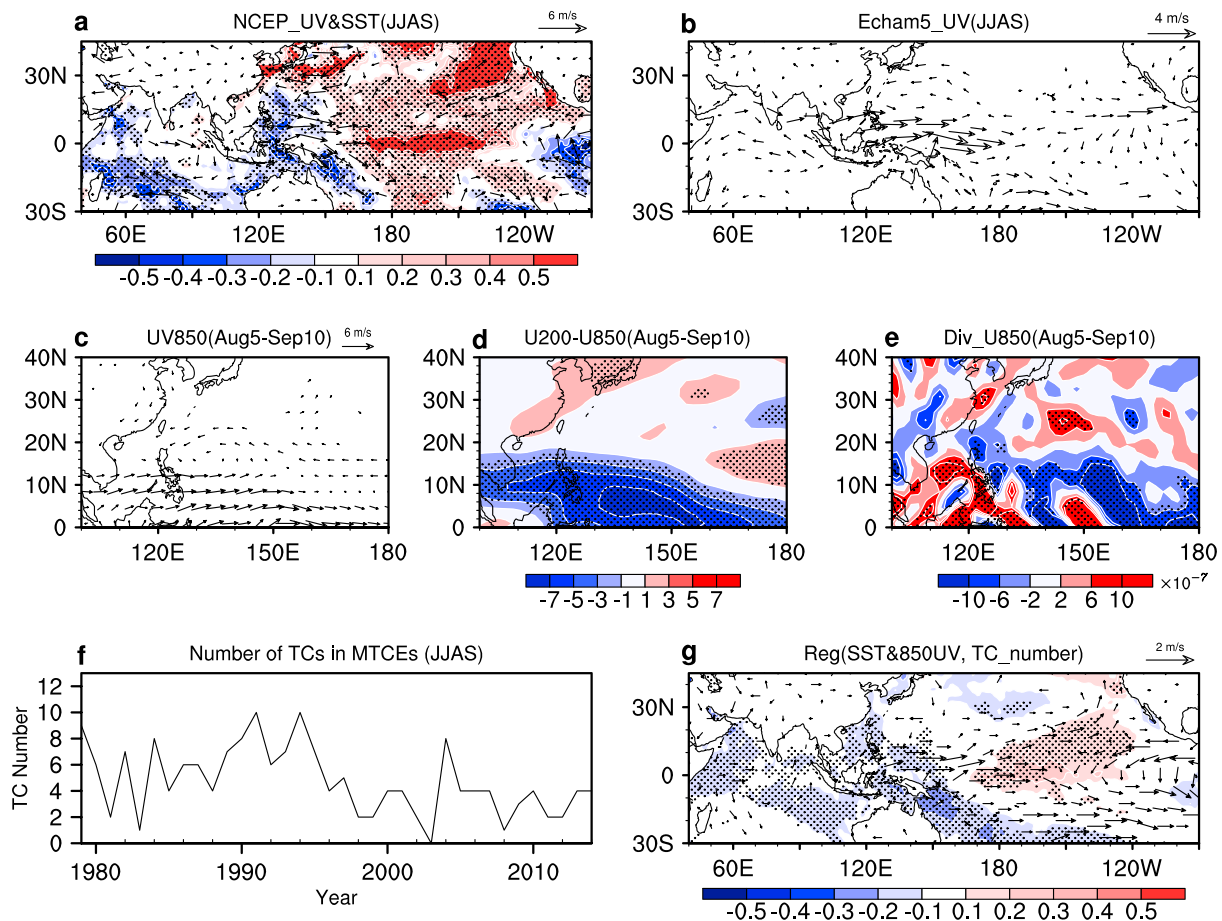
Figure 4. Relationship between SST and MTCEs. (a) Departure of JJAS mean SST (colors; K) and 850-hPa winds (arrows; m/s) in 2004 from the climatology (1979–2014). (b) Composite difference in JJAS mean 850-hPa winds (m/s) between EXP1 and EXP2. (c–e) Composite difference between EXP1 and EXP2 of, respectively, the mean 850-hPa winds (m/s), zonal vertical shear (colors; m/s), and 850-hPa zonal divergence (colors; s^{-1}) during 5 August to 10 September between EXP1 and EXP2, respectively. (f) The number of TCs in MTCEs in JJAS during 1979–2014. (g) The regression of JJAS SST (colors; K) and 850-hPa winds (arrows; m/s) on the number of TCs in MTCEs during 1979–2014. Only wind vectors passing 95% confidence level are shown, and shading denotes the anomalies shown by colors passing 95% confidence level. A 2000-sample bootstrap test is used in (a), (c), (d) and (e), while a two-tailed Student's t test is applied in (b) and (g). SST = sea surface temperature; MTCE = multiple tropical cyclogenesis event; JJAS = June to September; TC = tropical cyclone; NCEP = National Centers for Environmental prediction.

distance is based on the result by Shi et al. (2016) that the TCED-induced TC forms in the east or southwest directions at distances ranging from 1,000 to 3,500 km. Compared to the method used by Krouse and Sobel (2010), the criteria adopt a relatively short cutoff distance and moreover take the TCED signature into account to consider TCED process to identify MTCEs.

Using this method, we calculate the number of TCs in MTCEs for each typhoon season (Figure 4f). The regression of JJAS SST (Figure 4g) upon the normalized annual number of TCs in MTCEs during 1979–2014 also features significant positive SST anomalies in the tropical central Pacific and negative anomalies in the tropical Indian Ocean. Consistent with the regressed SST pattern, the regressed JJAS 850-hPa winds onto the normalized number of TCs in MTCEs (Figure 4g) display a strengthened monsoon trough over the NWP as well. Both the regressed SST and 850-hPa wind patterns (Figure 4g) are very similar to those observed in the JJAS of 2004 (Figure 4a), indicating that the anomalous SST pattern increases the possibility of MTCE.

Specifically, the regressed SST pattern resembles that associated with an El Niño Modoki event (Ashok et al., 2007) to a certain extent, which is considered to facilitate the development of a monsoon trough in the NWP (Chen & Tam, 2010; Mei et al., 2015). The correlation between the JJAS El Niño Modoki index (Ashok et al., 2007) and the number of TCs in MTCEs is as high as 0.57 (above the 99% confidence level) during 1979–2014.

4. Conclusions

The development of the train-like MTCE can be summarized as follows. In the summer of 2004, an El Niño Modoki-like SST pattern with positive anomalies in the tropical central Pacific and negative anomalies in the tropical Indian Ocean likely caused a long-lasting monsoon trough over the NWP. A strong typhoon (Rananim) emitted a Rossby wave packet energy into the monsoon trough. The monsoon trough appears to help the Rossby wave-induced cyclonic disturbances evolve into the following new TCs. In this way, seven TCs were generated in sequence, forming the extreme train-like MTCE.

An analysis of the historical record from 1979 to 2014 also shows that an El Niño Modoki-like SST pattern likely increases the possibility of MTCEs. The link between the SST pattern and MTCEs may help to predict an extreme MTCE occurrence. As the El Niño Modoki event is projected to occur more frequently under the projected global warming scenarios (Yeh et al., 2009), such extreme MTCEs may become more common as well.

References

Ashok, K., Behera, S. K., Rao, S. A., Weng, H. Y., & Yamagata, T. (2007). El Niño Modoki and its possible teleconnection. *Journal of Geophysical Research*, *112*, C11007. https://doi.org/10.1029/2006JC003798

Atlas, R., Hoffman, R. N., Ardizzone, J., Leidner, S. M., Jusem, J. C., Smith, D. K., & Gombos, D. (2011). A cross-calibrated, multiplatform ocean surface wind velocity product for meteorological and oceanographic applications. *Bulletin of the American Meteorological Society*, *92*(2), 157–174. https://doi.org/10.1175/2010BAMS2946.1

Camargo, S. J., Emanuel, K. A., & Sobel, A. H. (2007). Use of a genesis potential index to diagnose ENSO effects on tropical cyclone genesis. *Journal of Climate*, *20*(19), 4819–4834. https://doi.org/10.1175/JCLI4282.1

Chan, J. C. L., & Williams, R. (1987). Analytical and numerical studies of the beta-effect in tropical cyclone motion. I: Zero mean flow. *Journal of the Atmospheric Sciences*, *44*(9), 1257–1265. https://doi.org/10.1175/1520-0469(1987)044<1257:AANSOT>2.0.CO;2

Chen, G., & Tam, C.-Y. (2010). Different impacts of two kinds of Pacific Ocean warming on tropical cyclone frequency over the western North Pacific. *Geophysical Research Letters*, *37*, L01803. https://doi.org/10.1029/2009GL041708

Duchon, C. E. (1979). Lanczos filtering in one and two dimensions. *Journal of Applied Meteorology*, *18*(8), 1016–1022. https://doi.org/10.1175/1520-0450(1979)018<1016:LFIOAT>2.0.CO;2

Fu, B., Li, T., Peng, M. S., & Weng, F. (2007). Analysis of tropical cyclogenesis in the western North Pacific for 2000 and 2001. *Weather and Forecasting*, *22*(4), 763–780. https://doi.org/10.1175/WAF1013.1

Gao, J., & Li, T. (2011). Factors controlling multiple tropical cyclone events in the western North Pacific. *Monthly Weather Review*, *139*(3), 885–894. https://doi.org/10.1175/2010mwr3340.1

Ge, X., Li, T., & Zhou, X. (2007). Tropical cyclone energy dispersion under vertical shears. *Geophysical Research Letters*, *34*, L23807. https://doi.org/10.1029/2007GL031867

Gray, W. (1979). Hurricanes: Their formation, structure and likely role in the tropical circulation. In D. B. Shaw (Ed.), *Meteorology over the tropical oceans* (pp. 155–218). Bracknell, UK: Royal Meteorological Society.

Hodges, K., Chappell, D., Robinson, G., & Yang, G. (2000). An improved algorithm for generating global window brightness temperatures from multiple satellite infrared imagery. *Journal of Atmospheric and Oceanic Technology*, *17*(10), 1296–1312. https://doi.org/10.1175/1520-0426(2000)017<1296:AIAFGG>2.0.CO;2

Holland, G. (1995). Scale interaction in the western Pacific monsoon. *Meteorology and Atmospheric Physics*, *56*(1-2), 57–79. https://doi.org/10.1007/BF01022521

Johnson, R. W. (2001). An introduction to the bootstrap. *Teaching Statistics*, *23*(2), 49–54. https://doi.org/10.1111/1467-9639.00050

Kanamitsu, M., Ebisuzaki, W., Woollen, J., Yang, S. K., Hnilo, J., Fiorino, M., & Potter, G. (2002). NCEP-DOE AMIP-II reanalysis (R-2). *Bulletin of the American Meteorological Society*, *83*(11), 1631–1644. https://doi.org/10.1175/BAMS-83-11-1631

Kim, J. H., Ho, C. H., & Sui, C. H. (2005). Circulation features associated with the record-breaking typhoon landfall on Japan in 2004. *Geophysical Research Letters*, *32*, L14713. https://doi.org/10.1029/2005GL022494

Knapp, K. R., Kruk, M. C., Levinson, D. H., Diamond, H. J., & Neumann, C. J. (2010). The international best track archive for climate stewardship (IBTrACS). *Bulletin of the American Meteorological Society*, *91*(3), 363–376. https://doi.org/10.1175/2009bams2755.1

Krouse, K. D., & Sobel, A. H. (2010). An observational study of multiple tropical cyclone events in the western north Pacific. *Tellus A*, *62*(3), 256–265. https://doi.org/10.1111/j.1600-0870.2010.00435.x

Krouse, K. D., Sobel, A. H., & Polvani, L. M. (2008). On the wavelength of the Rossby waves radiated by tropical cyclones. *Journal of the Atmospheric Sciences*, *65*(2), 644–654. https://doi.org/10.1175/2007JAS2402.1

Lau, K. H., & Lau, N. C. (1992). The energetics and propagation dynamics of tropical summertime synoptic-scale disturbances. *Monthly Weather Review*, *120*(11), 2523–2539. https://doi.org/10.1175/1520-0493(1992)120<2523:TEAPDO>2.0.CO;2

Li, T., & Fu, B. (2006). Tropical cyclogenesis associated with Rossby wave energy dispersion of a preexisting typhoon. Part I: Satellite data analyses*. *Journal of the Atmospheric Sciences*, *63*(5), 1377–1389. https://doi.org/10.1175/JAS3692.1

Mei, W., Xie, S., Zhao, M., & Wang, Y. (2015). Forced and internal variability of tropical cyclone track density in the western North Pacific. *Journal of Climate*, *28*(1), 143–167. https://doi.org/10.1175/JCLI-D-14-00164.1

Molinari, J., Lombardo, K., & Vollaro, D. (2007). Tropical cyclogenesis within an equatorial Rossby wave packet. *Journal of the Atmospheric Sciences*, *64*(4), 1301–1317. https://doi.org/10.1175/JAS3902.1

Nakazawa, T. (2006). Madden-Julian Oscillation activity and typhoon landfall on Japan in 2004. *Solaiat*, *2*, 136–139. https://doi.org/10.2151/sola.2006-035

Rayner, N. A., Parker, D. E., Horton, E. B., Folland, C. K., Alexander, L. V., Rowell, D. P., et al. (2003). Global analyses of sea surface temperature, sea ice, and night marine air temperature since the late nineteenth century. *Journal of Geophysical Research*, *108*(D14), 4407. https://doi.org/10.1029/2002JD002670

Roesch, A., & Roeckner, E. (2006). Assessment of snow cover and surface albedo in the ECHAM5 general circulation model. *Journal of Climate*, *19*(16), 3828–3843. https://doi.org/10.1175/JCLI3825.1

Schenkel, B. A. (2016). A climatology of multiple tropical cyclone events. *Journal of Climate*, *29*(13), 4861–4883. https://doi.org/10.1175/JCLI-D-15-0048.1

Schenkel, B. A. (2017). Are multiple tropical cyclone events similar among basins? *Journal of Climate*, *30*(15), 5805–5813. https://doi.org/10.1175/JCLI-D-17-0088.1

Shi, W., Fei, J., Huang, X., Liu, Y., Ma, Z., & Yang, L. (2016). Rossby wave energy dispersion from tropical cyclone in zonal basic flows. *Journal of Geophysical Research: Atmospheres*, *121*, 3120–3138. https://doi.org/10.1002/2015JD024207

Shi, W., Fei, J., Huang, X., & Ma, Z. (2017). Where will tropical cyclogenesis occur around a preexisting tropical cyclone? *Geophysical Research Letters*, *44*, 578–586. https://doi.org/10.1002/2016GL072157

Trenberth, K. E. (1986). An assessment of the impact of transient eddies on the zonal flow during a blocking episode using localized Eliassen-Palm flux diagnostics. *Journal of the Atmospheric Sciences*, *43*(19), 2070–2087. https://doi.org/10.1175/1520-0469(1986)043<2070:AAOTIO>2.0.CO;2

Wang, B., Wu, R. G., & Li, T. (2003). Atmosphere-warm ocean interaction and its impacts on Asian-Australian monsoon variation. *Journal of Climate*, *16*(8), 1195–1211. https://doi.org/10.1175/1520-0442(2003)16<1195:AOIAII>2.0.CO;2

Webster, P. J., & Chang, H. R. (1988). Equatorial energy accumulation and emanation regions: Impacts of a zonally varying basic state. *Journal of the Atmospheric Sciences*, *45*(5), 803–829. https://doi.org/10.1175/1520-0469(1988)045<0803:EEAAER>2.0.CO;2

Wheeler, M. C., & Hendon, H. H. (2004). An all-season real-time multivariate MJO index: Development of an index for monitoring and prediction. *Monthly Weather Review*, *132*(8), 1917–1932. https://doi.org/10.1175/1520-0493(2004)132<1917:AARMMI>2.0.CO;2

Xie, S. P., Hu, K. M., Hafner, J., Tokinaga, H., Du, Y., Huang, G., & Sampe, T. (2009). Indian Ocean capacitor effect on Indo-Western Pacific climate during the summer following El Niño. *Journal of Climate*, *22*(3), 730–747. https://doi.org/10.1175/2008JCLI2544.1

Xu, Y., Li, T., & Peng, M. S. (2013). Tropical cyclogenesis in the western North Pacific as revealed by the 2008–09 YOTC data*. *Weather and Forecasting*, *28*(4), 1038–1056. https://doi.org/10.1175/WAF-D-12-00104.1

Yeh, S., Kug, J., Dewitte, B., Kwon, M., Kirtman, B. P., & Jin, F. (2009). El Niño in a changing climate. *Nature*, *461*(7263), 511–514. https://doi.org/10.1038/nature08316